Fish and Shellfish Immunology 90 (2019) 188–198

Contents lists available at ScienceDirect

Fish and Shellfish Immunology

journal homepage: www.elsevier.com/locate/fsi

Full length article

C-type lectin response to bacterial infection and ammonia nitrogen stress in tiger shrimp (*Penaeus monodon*)

Yukai Qin[a,b], Shigui Jiang[a,c], Jianhua Huang[a,c], Falin Zhou[a,c], Qibin Yang[a,c], Song Jiang[a,c], Lishi Yang[a,c,*]

[a] South China Sea Fisheries Research Institute, Chinese Academy of Fishery Sciences, Key Laboratory of South China Sea Fishery Resources Exploitation and Utilization, Ministry of Agriculture, Guangzhou, 510300, PR China
[b] College of Aqua-life Science and Technology, Shanghai Ocean University, Shanghai, PR China
[c] Shenzhen Base of South China Sea Fisheries Research Institute, Chinese Academy of Fishery Sciences, Shenzhen, 518108, PR China

ARTICLE INFO

Keywords:
Penaeus monodon
C-type lectins
Pattern recognition receptor
Innate immunity
Ammonia nitrogen

ABSTRACT

C-type lectins (CTLs) are pattern recognition receptors (PRRs) that are important in invertebrate innate immunity for the recognition and elimination of pathogens. Although they were reported in many shrimp, C-type lectins subfamily contain a large number of members with different functions that need to research in deep. In this present study, a new type of CTL, PmCL1 with 861 bp long full-length cDNA, that encodes a protein with 164-amino acid from a 495-bp open reading frame, was isolated and characterized from tiger shrimp (*Penaeus monodon*). The mRNA transcript of PmCL1 showed the highest expression in the hepatopancreas, whereas it was barely detected in the ovary. After the shrimp were stimulated by *Vibrio harveyi* and *Vibrio anguillarum*, PmCL1 expression in the hepatopancreas and gill was significantly upregulated. A carbohydrate-binding assay revealed the specificity of PmCL1 for pathogen-associated molecular patterns (PAMPs) that included peptidoglycan (PGN) and lipopolysaccharide (LPS), and saccharides that included D-glucose, galactosamine, α-lactose, treholose, and D-mannose. Recombinant PmCL1 agglutinated gram-positive (*Staphylococcus aureus*) and gram-negative bacteria (*V. harveyi*, *V. anguillarum*, *Vibrio alginolyticus*, *Vibrio parahemolyticus*, *Vibrio vulnificus*, and *Aeromonas hydrophila*) in the presence of calcium ions and enhanced the efficiency of clearing the invading bacteria. Collectively, our results suggested that PmCL1 might play an important role as a pattern recognition receptor (PRR) in the immune response towards pathogen infections, as well as the response towards ammonia nitrogen stress.

1. Introduction

Invertebrate defence against pathogens depends on innate immunity, owing to the absence of acquired immunity [1,2]. Many proteins are known to participate in the innate immune response, including pattern recognition receptors (PRRs), which are germline-encoded host sensors that detect molecules typical of pathogens, termed as pathogen-associated molecular patterns (PAMPs) [3]. PAMPs include bacterial cell wall components such as lipopolysaccharide (LPS), peptidoglycan (PGN), and β-1, 3-glucans, which can be recognized by PRRs [3] such as Toll-like receptors (TLRs) [4,5], scavenger receptors (SCRs) [6], and lectins [7–9] to facilitate pathogen recognition (including their endogenous components), phagocytosis, pathogen elimination, and numerous other biological processes [10,11].

Lectins, as a number of PRRs, play an important role in innate immunity of invertebrate, especially in crustacean. Lectins are divided into many groups based on specific motifs, including C-type, F-type, I-type, L-type, M-type, P-type, R-type, chitinase-like lectins, ficolins, calnexin, galectins, and intelectins [11]. Among these, the C-type lectins (CTLs) have been widely studied. The main characteristic of the CTL superfamily of proteins is the presence of a carbohydrate recognition domain (CRD) composed of approximately 115–130 amino acids, with several conserved motifs. CRDs consist of four cysteine residues, which form two disulphide bridges, located at the base of two highly conserved loops [12]. CTLs bind carbohydrates with the participation of calcium ions (Ca^{2+}) [13], and play an important in many physiological and biochemical processes, besides serving as PRRs. These roles include cell adhesion [14], activation of prophenoloxidase [15], microbial agglutination [16], phagocytosis [17], and encapsulation. *PcLec3* from crayfish (*Procambarus clarkii*) is upregulated in the hepatopancreas upon challenge with *Vibrio anguillarum*, whereas no obvious change occurs after a challenge with white spot syndrome virus

* Corresponding author. South China Sea Fisheries Research Institute, Chinese Academy of Fishery Sciences, 231 Xingang West Road, Guangzhou, 510300, China.
E-mail address: lishi_yang@yahoo.com (L. Yang).

https://doi.org/10.1016/j.fsi.2019.04.034
Received 3 November 2018; Received in revised form 26 March 2019; Accepted 11 April 2019
Available online 24 April 2019
1050-4648/

(WSSV) [18]. *SpCTL-B* [19] transcripts from mud crab (*Scylla paramamosain*) are significantly increased in the hepatopancreas and haemocytes after stimulation by LPS, *V. parahemolyticus*, and WSSV. *PtCTL4* [20], *EsCTLDcp* [21], and *MnCTLDcp1* [22] can facilitate the adhesion and aggregation of microorganisms. At the same time, some CTLs have also been reported in black tiger shrimp (*Penaeus monodon*), including *PmLec* [23], which shows a strong haemagglutinating and bacterial-agglutinating activity, *PmLT* [24], with two CRDs that show a strong response to white spot syndrome virus (WSSV) extract, and *PmCLec* [25], which shows agglutination activity with gram-positive bacteria but does not bind gram-negative bacteria.

The black tiger shrimp (*Penaeus monodon*) is a commercially significant crustacean species that is widely cultured on the southern coast of China. However, many diseases caused by pathogens including virus, bacteria, and fungus threaten the shrimp culture industry. Research into the mechanism of innate immune response underlying the defence towards pathogens is urgently needed to improve the immunity of shrimp. Meanwhile, water pollution by overfeeding is also shaping up to be a serious problem. Among the multiple pollutants of water, ammonia nitrogen is a particularly common toxin, which is considered the main limiting factor that can rapidly cause increased shrimp mortality and severe economic losses [26–30]. Some previous studies have reported that ammonia nitrogen stress reduced the immunity of aquatic animals by inhibiting the activity of superoxide dismutase (SOD) and phenoloxidase, as well as phagocytosis [31–33]. Transcriptome analyses have revealed that many immune related genes, including C-type lectin, lysozyme, and serine proteinase inhibitors, are enriched significantly [34] under acute ammonia stress. However, additional data and further detailed analysis are needed for a comprehensive verification of the association between ammonia nitrogen stress and CTLs.

In the present study, we identified a novel CTL, designated PmCL1, using a formal transcriptome database constructed in our lab. Expression profiles analysis revealed the role of PmCL1 in response to various immune challenges and ammonia nitrogen. Furthermore, the recombinant PmCL1 (rPmCL1) had the ability of binding PAMPs and carbohydrates, as well as agglutinating gram-positive and gram-negative bacteria, enabling their removal *in vivo*.

2. Materials and methods

2.1. Construction of PmCL1 full-length cDNA

Based on the transcriptome of tiger shrimp hepatopancreas tissues, constructed in our laboratory (data not shown), we designed a pair of specific primers, PmCL1-F and PmCL1-R, to verify the detection specificity and accuracy of the PmCL1 sequence. The 5′ and 3′ ends of the mRNA were obtained by the rapid amplification of cDNA end (RACE) method (Clonetech, Japan). For 5′ or 3′ RACE-PCR, PCR was performed initially with PmCL1-rR1 (PmCL1-rF1 for 3′) and a universal primer, followed by semi-nested PCR with PmCL1-rR2 (PmCL1-rF2 for 3′) and a nested universal primer (Table 1). PCR conditions were as follows: one cycle of 94 °C for 3 min, 35 cycles of 94 °C for 30 s, 67 °C for 30 s, and 72 °C for 45 s, followed by a final cycle of 72 °C for 10 min. The PCR products were gel-purified, sequenced, and the resulting sequences were analysed.

2.2. Bioinformati analysis

The open reading frame (ORF)-finder and BLAST program from the National Center for Biotechnology Information server (NCBI; http://www.ncbi.nlm.nih.gov/) were used to analyse the sequences. Primer 5.0 was used to predict the amino acid sequences and design the related primers. ProtParam software (http://web. Expasy. org/protparam/) was used to deduce the amino acid sequences and predict protein physicochemical properties. The analysis of protein domains was done using the SMART4.0 online program (http://smart.embl-heidelberg.de/).The NetPhos2.0 program was used to predict the protein phosphorylation sites (http://www.cbs.dtu.dk/services/NetPhos/). Multiple sequence alignment and phylogenetic tree were constructed using Clustal X, BioEdit, and MEGA 6.0 software.

2.3. Experimental animals and collection of samples

Experimental black tiger shrimps (*P. monodon*) used for the experiments had an average weight of 15–18 g. All the animals were healthy, and were cultured at the Experimental Base of South China Sea Fisheries Research Institute (Shenzhen City, Guangdong Province, China). They were maintained in filtered aerated seawater at 28 ± 1 °C and fed daily with normal commercial bait.

Three tiger shrimp were sacrificed to collect tissues, including eyestalk, gill, brain, heart, hepatopancreas, abdominal ganglia, thoracic ganglia, lymph, intestines, stomach, ovary, testis, epidermis, and muscle. These 14 different tissues were immediately shred and stored in RNAlater® RNA Stabilization Solution (Invitrogen, USA).

2.4. Bacterial challenge and sample collection

Three bacterial strains were kindly provided by the Key Laboratory of South China Sea Fishery Resources Exploitation & Utilization. The bacteria were cultured in lysogeny broth (LB; 1% tryptone, 1% NaCl, and 0.5% yeast extract) at 30 °C for 12 h with constant shaking (220 rpm), and collected by centrifugation at 6000 × *g* for 5 min, following which, they were washed thrice with PBS and then suspended in PBS to 1.0×10^8 CFU/mL. In the lab record, the 96-h half-lethal concentration 50 (LC50) of *Staphylococcus aureus*, *Vibrio harveyi*, and *Vibrio anguillarum* were 1.5×10^9 CFU/mL, 2.0×10^8 CFU/mL, and 3.5×10^8 CFU/mL, respectively. Two hundred healthy juvenile *P. monodon*, with an average weight of 15–18 g, were used for immune challenge experiments. The shrimps were divided into four groups (n = 50 per group), with the first group serving as the control. They were injected with 100 μL sterile phosphate-buffered saline (PBS, pH 7.4). The shrimp in the other three groups individually received an injection of 100 μL (1.0×10^8 cfu/mL) of *S. aureus*, *V. harveyi*, or *V. anguillarum*, as described previously [35]. Each shrimp was injected intramuscularly in the second abdominal segment. The hepatopancreas and gill from at least three shrimps were sampled at 0, 3, 6, 9, 12, 24, 48, and 72 h following the injection. The tissues were stored in RNAlater at −80 °C until RNA extraction.

2.5. Ammonia nitrogen stress

Based on the previous experimental results from our laboratory, a 96-h acute ammonia toxicity experiment was done, which yielded a 96-h safe concentration 50 (SC50) and a 96-h half-lethal concentration 50 (LC50) of 6.5 mg/L NH_4Cl and 65 mg/L NH4Cl, respectively. Next, 120 healthy shrimps were randomly allocated for two treatments, including a 96-h SC50 concentration and 96-h LC50 concentration, with the shrimp in natural seawater without stimulation serving as the control. The temperature, pH, and salinity of the seawater were maintained at 29 ± 0.5 °C, 7.5 ± 0.5, and 29%–30%, respectively. Half the volume in the experimental tanks was replaced every 12 h. No food was supplied during the experiment. Survival of the shrimps was recorded every 2 h. Dead shrimps were immediately removed by siphoning. Four shrimps were collected at 0, 3, 6, 12, 24, 48, 72, and 96 h after the establishment of ammonia nitrogen stress. Hepatopancreas and intestine tissue samples collected from the shrimps were immediately shred and stored in RNAlater (Invitrogen, USA) at −80 °C until use for RNA extraction.

2.6. Total RNA isolation and cDNA synthesis

Total RNA from all the samples collected above was extracted using

Table 1
PCR primers used in the experiment.

Primer	Primer sequence (5′–3′)	Purpose
PmCL1- F PmCL1- R	TCACTCTTCCAAGGGACTGC GATATTGCAGCCATCCAGAAG	ORF Validation
PmCL1-rR1 PmCL1-rR2	CGTAACCGTTCTTGTCGCACTCGC CAGAGAGGAATCCCCATCTTCACGG	5′RACE
PmCL1-rF1 PmCL1-rF2	GAAGATGGGGATTCCTCTCTGGGG GGCGAGTGCGACAAGAACGGTTAC	3′RACE
UPM-long UPM-short Nested Primer	CTAATACGACTCACTATAGGGCAAGCAGTGGTATCAACGCAGAGT CTAATACGACTCACTATAGGGC AAGCAGTGGTATCAACGCAGAGT	Universal Primer
PmCL1-qF PmCL1-qR	AGAACAAGTGCTACTACT TTACGAGAAGGCTGAATT	q RT-PCR
EF-1α-qF EF-1α-qR	AAGCCAGGTATGGTTGTCAACTTT CGTGGTGCATCTCCACAGACT	Reference gene
PmCL1-32a-F PmCL1-32a-R	CGCG^GATCCCTGTGTCCTGAGCCTTTCG CGC^TCGAGTTAGATCAGGCAGAGGGTCGATC	Prokaryotic expression

Trizol Reagent (Invitrogen, USA), following the manufacturer's directions. The quantity of extracted RNA was determined by measuring the ratio of ultraviolet absorbance at 260/280 nm using a NanoDrop 2000 device (NanoDrop Technologies, USA). Integrity was ensured by 1.5% agarose gel electrophoresis. A total of 2 μg RNA from the hepatopancreas, muscle, and haemocytes was synthesized using the PrimeScript II 1st Strand cDNA Synthesis Kit (Takara, Japan). For real-time quantitative PCR (q RT-PCR), the cDNA was synthesized followed the manufacturer's instructions for the PrimeScript ™ RT Reagent Kit with gDNA Eraser (Perfect Real-time, Takara, Japan), and diluted to 50 ng/μL for use as the template.

2.7. Real-time RT-PCR analysis of PmCL1 mRNA expression

Real-time qRT-PCR was used to detect the mRNA expression of PmCL1 in different tissues after bacterial challenge and ammonia nitrogen. Elongation factor 1α (EF1α) was used as the reference gene (Table 1). The total volume of 12.5 μL in each well contained 6.25 μL of 2 × TB Green™ Premix ExTaq (Takara, Japan), 0.5 μL each of PmCL1-qF and PmCL1-qR, 1 μL of real-time PCR diluted cDNA, and 4.25 μL of double-distilled water. qPCR with green fluorescence measurement was carried out in a Roche Light Cycler® 480II with the following four steps: degeneration for 30 s at 95 °C, quantitative analysis stage with 40 cycles of 94 °C for 5 s and 60 °C for 30 s, dissolution curve analysis for 5 s at 95 °C, 1 min at 60 °C, and 95 °C, and a cooling stage of 30 s at 50 °C. The PCR data were obtained using the relative CT method ($2^{-\Delta\Delta CT}$ method). Statistical analyses were performed using one-way ANOVA, followed by Tukey's multiple range test, using SPSS statistics version 23.0 software (IBM, USA). The differences were considered to significant for $P < 0.05$. Test data are shown as means ± standard error (mean ± SE).

2.8. Expression and purification of recombinant PmCL1 (rPmCL1)

The 135 amino acid cDNA fragment of PmCL1 without a signal peptide sequence was amplified with specific primers containing *Bam*H I and *Xho*I sites (underline) at their 5′ end. The cDNA fragment was subcloned into the pET32a (+) plasmid and transformed into *Escherichia coli* Rosseta (DE3). Positive clones were confirmed by nucleotide sequencing. The positive transformants and negative control were both grown in 300 mL LA medium (100 μg/mL ampicillin) at 37 °C and 220 rpm for 12 h, to an optical density of 0.6 at 600 nm (OD600). Thereafter, the expression of recombinant protein was induced by treatment with 0.5 mM isopropyl-β-D-thio-galactoside for 6 h at 28 °C.

Cells were harvested by centrifugation at 7000 × *g* for 15 min at 4 °C, and then suspended in 1 × PBS (137 mM NaCl, 2.7 mM KCl, 10 mM Na_2HPO_4, 2 mM KH_2PO_4, pH 7.4). The suspension was sonicated on ice for 20 min, using 4 s sonication and 7 s interval at 60% power (JY92-IIDN, China). The cellular debris was centrifuged at 10,000 × *g* for 10 min at 4 °C. The supernatant was added to Ni-NTA His Bind Resin (Invitrogen, USA) to obtain purified protein, as instructed by the manufacturer. The target protein was checked by an anti-His-tag, using the previously described Western blot protocol [36].

2.9. Assay for the binding of PAMPs and saccharides

To detect the direct binding ability of rPmCL1, three types of PAMPs (LPS, LTA, and PGN) and five types of carbohydrates (D-mannose, D-glucose, galactosamine, lactose, and treholose) were detected by enzyme-linked immunosorbent assay (ELISA). Each PAMP or carbohydrate was dissolved in water to achieve a concentration of 100 mg/mL, before addition to each well of a microtiter plate. The PAMPs and carbohydrates were maintained at 4 °C for 24 h, and each well of the plate was blocked with 200 mL of 5% bovine serum albumin (BSA) at 37 °C for 40 min. The plates were washed thrice with PBS containing 3% Tween-20 (PBST), and a 100-μL volume of various concentrations of recombinant protein (0–150 μg/mL dissolved in PBS) was added to the wells. The plate was incubated at 37 °C for 40–60 min and then washed three times. Monoclonal His-tag antibody (1:5000 dilution) was added to each well and incubated at 37 °C for 1 h. The plate was washed thrice as described above and developed with times before the addition of 0.01% 3,3′,5,5′-tetramethylbenzidine (TMB, Sigma-Aldrich, USA). The reaction was stopped by adding 2 M H_2SO_4 and the absorbance was recorded at 450 nm. All the assays were performed in triplicate. For the control, BSA was used instead of rPmCL1.

2.10. Agglutination assay

A gram-positive bacterium (*S. aureus*) and 6 g-negative bacteria (*V. harveyi*, *V. anguillarum*, *V. alginolyticus*, *V. parahemolyticus*, *V. vulnificus*, and *Aeromonas hydrophila*) were used to measure the binding activity of rPmCL1, via a binding assay. After cultivation, the bacteria were harvested by centrifugation at 12,000 × *g* for 2 min, washed thrice using PBS, and suspended to an approximate density of 1×10^8 cfu/mL in PBS-Ca^{2+} buffer (10 mM $CaCl_2$ in 1 × PBS, pH 7.4). A 25-μL volume of the prepared bacterial suspension was incubated with 25 μL of 100 μg/mL rPmCL1 or BSA at 25 °C for 1 h, with gentle rotation in coated wells. To examine the effect of ethylene diamine tetraacetic acid (EDTA), 20 mM EDTA was added to the PBS-Ca^{2+} buffer, and the assay was performed as described above. To determine the sugar-binding specificity of rPmCL1, 25 μL of the protein was mixed with an equal volume of 100 μg/mL PGN. The mixtures were incubated at 25 °C for 1 h and then added to 25 μL of bacterial suspension, prepared as described above. Agglutination was observed under an optical microscope.

2.11. Bacterial clearance assay in vivo

A total of 30 black tiger shrimp, with an average weight of 15–18 g, were randomly divided into three groups and cultured in sea water tanks for 3 days before the experiment. Overnight cultured *V. harveyi* was harvested and suspended to an approximate density of 1×10^7 cfu/mL in PBS. Purified rPmCL1 (500 μL, 500 μg/mL) in PBS was incubated with 500 μL of *V. harveyi* at 28 °C for 30 min, with gentle rotation. The bacteria were incubated with 500 μL 5% BSA or 1 × PBS as the positive control. Each shrimp was injected with a 50-μL mixture, and shrimp haemolymph (500 μL) was extracted in tubes containing 500 μL ice-cold ACD anticoagulant buffer (1.32% sodium citrate, 0.48% citric acid, 1.47% glucose) at 5, 15, and 30 min post-injection. The plasma was obtained by centrifugation at 5000 rpm for 5 min, and then serially diluted with PBS. Aliquots (100 μL each) of plasma were plated on LB agar. Bacteria were enumerated after overnight culturing at 28 °C.

3. Results

3.1. cDNA cloning and characterization of PmCL1 gene

The 453-bp partial sequence of PmCL1 was obtained from the transcriptome data of the hepatopancreas of black tiger shrimp. RACE revealed a complete cDNA sequence of PmCL1 measuring 861 bp, including a 5′-untranslated region (5′-UTR) of 74 bp, an ORF of 495 bp, and a 292 bp 3′-UTR with a poly(A) tail (Fig. 1). The sequence has been deposited in GenBank under accession number MK076295. The ORF encoded a 164 amino acid polypeptide with a deduced molecular (without a signal peptide) weight of 16.17 kDa and a theoretical isoelectric point of 4.42.

Prediction of phosphorylation sites using the NetPhos 3.1 Server revealed that the deduced amino acid of PmCL1 had nine phosphorylation sites, including five serine residues, three threonine residues, and one tyrosine (Fig. 1). No glycosylation sites were predicted in the sequence by the NetNGlyc 1.0 Server. The deduced amino acid sequence contained a signal peptide of 20 amino acids, with an ATG initiation codon and a single typical CRD of C-type lectin, which had a typical carbohydrate-binding motif formed by three sequential amino acids (E123, P124, and S125) and six highly conserved cysteine residues (C22, C33, C51, C132, C149, and C156).

3.2. Multiple sequence alignment and phylogenetic tree analysis

Multiple sequence alignment analysis of PmCL1 against the CTLs from various species revealed different amino acid compositions (Fig. 2A). Sequence analysis using the BLASTX program and the Clustal X 2.1 software revealed that the amino acid of PmCL1 was similar to the CTLs from *Scylla paramamosain* (AEO92002.1, 55% similarity), *Portunus trituberculatus* (ACC86854.1, 54% similarity), and *P. japonicus* (ADG85661.1, 51% similarity). All the conserved cysteine residues involved in formation of disulphide bridges were found to be present. The results of multiple alignments were used to construct a phylogenetic tree by neighbour-joining using MEGA6.0 software (Fig. 2B). The lectin proteins were divided into branches with similar sugar-binding motifs, whereas PmCL1 had a different EPS motif that formed a monophyletic clade in the phylogenetic tree (Fig. 2B). PmCL1 close with the branch including Pmlec from *P. monodon*, lectins from *E. sinensis*.

3.3. Tissue distribution of PmCL1 transcripts

The expression pattern of PmCL1 was detected by qRT-PCR, using EF1α as a control, in various tissues including the hepatopancreas, heart, lymph, gill, epidermis, stomach, ventral nerves, muscle, spermataphore sac, intestine, eyestalk nerves, testis, brain nerves, and ovary. PmCL1 was constitutively distributed in all the tested tissues. In particular, the highest expression was detected in the hepatopancreas, which showed a nearly 3000-fold higher expression than that in the ovary. In addition, the transcription of PmCL1 was also high in the heart and lymph, with significantly ($P < 0.05$) higher levels than those in other tested tissues. Expression of the gene was low in stomach, ventral nerves, muscle, spermataphore sac, intestine, eyestalk nerves, testis, and brain nerves, and was barely detectable in the ovary tissue (Fig. 3).

3.4. Transcription analysis of PmCL1 after bacterial challenge

Two gram-negative bacteria (*V. harveyi* and *V. anguillarum*) and a gram-positive bacterium (*S. aureus*) were separately injected into shrimp to test the PmCL1 expression level after immune challenge. The mRNA expression of PmCL1 in the shrimp hepatopancreas after the bacterial challenge is presented in Fig. 4A and B. PmCL1 was visually more sensitive to *V. anguillarum* than towards *S. aureus* and *V. harveyi* in the hepatopancreas and gill. In gills, the PmCL1 transcript levels were marginally decreased in the PBS and gram-positive groups, showing a significant difference from the gram-negative groups. In the *V. harveyi* group, the transcription of PmCL1 were upregulated at 9 h, peaked at 24 h, and was reduced thereafter, but remained higher than the value at 0 h (2.66-fold). However, the expression of PmCL1 in the *V. anguillarum* group peaked at 6 h and decreased thereafter, but remained significantly higher than the value at 0 h (5.07-fold). In hepatopancreas, the transcripts of PmCL1 were downregulated at 6 h in the PBS group (0.79-fold compared to 0 h) and the gram-positive group (0.82-fold compared to 0 h). PmCL1 expression was increased at 6 h in the *V. harveyi* and *V. anguillarum* groups; the elevated expression was maintained and peaked at 12 h (4.63-fold compared to 0 h) and 24 h (2.61-fold compared to 0 h), respectively. Transcript expression decreased at 48 h and 24 h, respectively, and returned to normal levels at 72 h. The results indicated that PmCL1 might be more sensitive in hepatopancreas injected with *V. anguillarum* compared with the *V. harveyi* group, with a shorter response time, which was significantly different compared with the gill.

3.5. Transcription analysis of PmCL1 under ammonia nitrogen stress

The SC and LC groups were set as models of low and high concentration of ammonia nitrogen stress, respectively, and the mRNA expression patterns of PmCL1 mRNA in hepatopancreas and intestines was fully analysed (Fig. 5). The results showed that the pattern of PmCL1 mRNA expression in the two groups had some similarities, as both declined under ammonia nitrogen, except the increase in the intestine of SC group. For hepatopancreas, the transcripts showed an immediate increase at 3 h (1.14-fold and 1.40-fold in the SC and LC group, respectively) and were subsequently reduced over 96 h in both SC group (0.77–0.47 fold) and LC group (0.74–0.44 fold). For intestine, the expression of PmCL1 in the SC group was upregulated at 3 h (4.43-fold) and stayed at a high expression (3.0–4.43 fold) until 96 h, whereas it increased at 3 h and decreased subsequently (0.67–0.24 fold) in the LC group.

3.6. Binding of rPmCL1 to PAMPs and carbohydrates

rPmCL1 was expressed in the soluble fraction of the Rosetta system after low temperature induction, and purified using Ni-NTA resin (Fig. 6). The observed molecular weight of rPmCL1 (~36 kD) was close to the predicted MW of the truncated protein without the signal peptide (35.6 kDa). The binding of purified rPmCL1 to PAMP was analysed by ELISA (Fig. 7). The binding of rPmCL1 to PGN was strong and occurred in a dose-dependent manner, with a high affinity evident at 50–100 μg/mL (absorbance of 0.175–0.202). The binding to LPS was evident, beginning at 25 μg/mL (absorbance 0.047) and increased slowly even at a higher concentration (150 μg/mL, absorbance 0.102). rPmCL1 did not display a binding activity to LTA at any concentration.

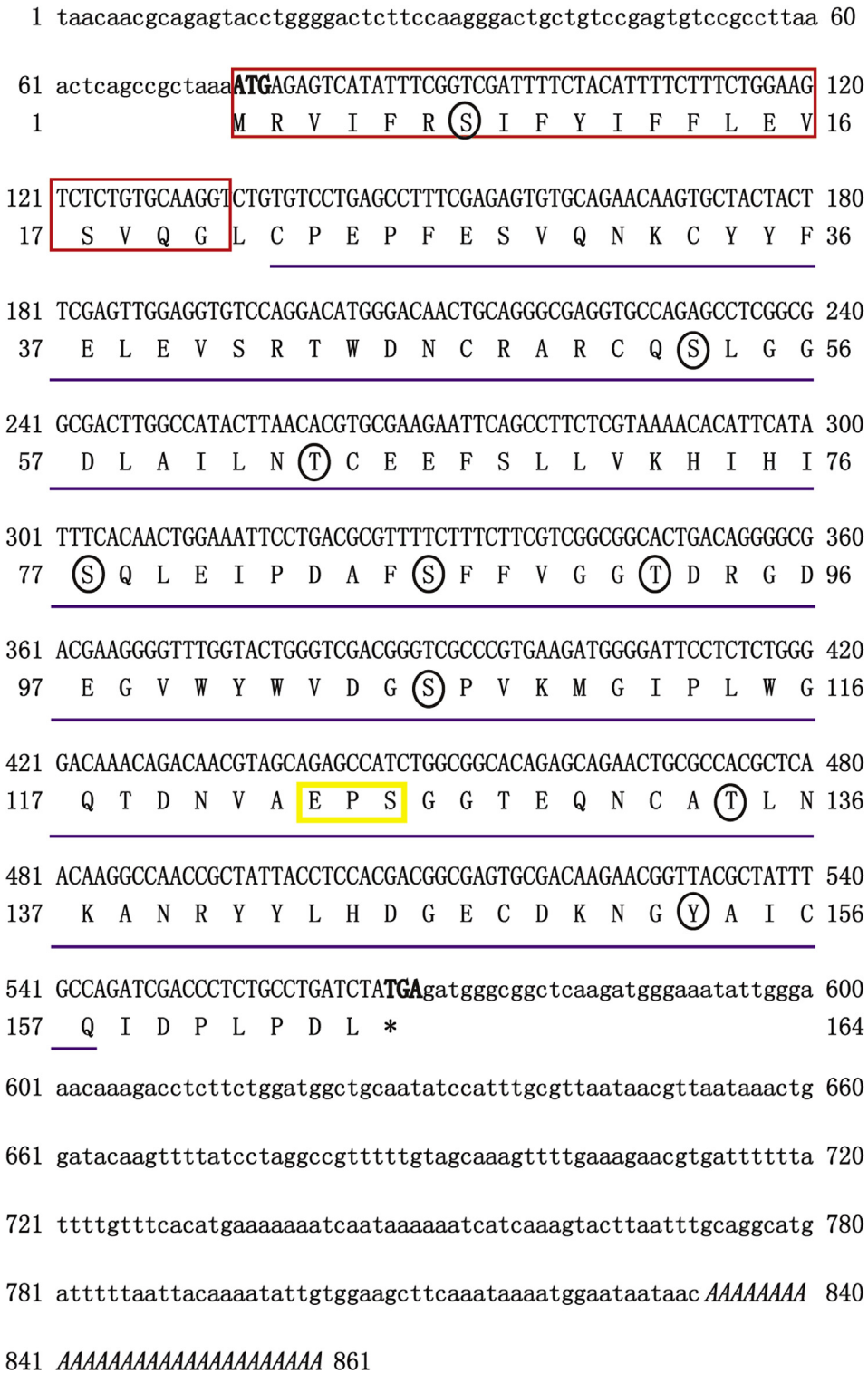

Fig. 1. Nucleotide sequence and deduced amino sequence of *PmCL1* from *Penaeus monodon*. The start and stop codons are marked in bold. A signal peptide sequence and sugar-binding motif are boxed. The CRD domain is underlined in purple. The phosphorylation sites are marked with circles. (For interpretation of the references to colour in this figure legend, the reader is referred to the Web version of this article.)

Similarly, the direct binding assay to carbohydrates revealed a rPmCL1 binding affinity that was similar for D-glucose and α-lactose, and marginally stronger for D-mannose, followed by galactosamine and trehalose. BSA did not bind with any of the carbohydrates.

3.7. Bacterial agglutination activity of rPmCL1

To determine whether the binding activity of the rPmCL1 protein could induce agglutination of bacteria, the protein was incubated with gram-positive (*S. aureus*) and gram-negative (*V. harveyi*, *V. anguillarum*, *V. alginolyticus*, *V. parahemolyticus*, *V. vulnificus*, and *A. hydrophila*) bacteria. Aggregation was clearly evident in all cases.

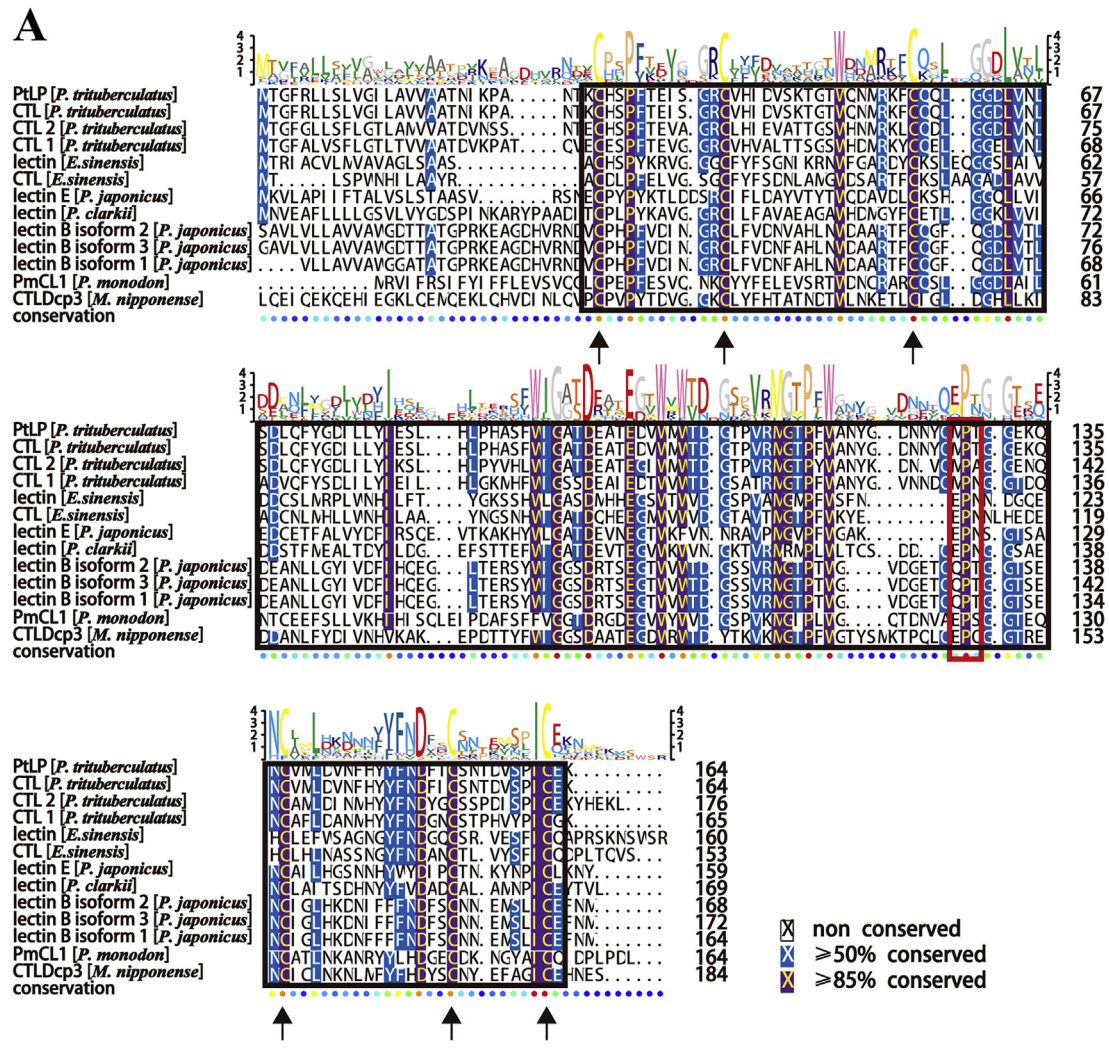

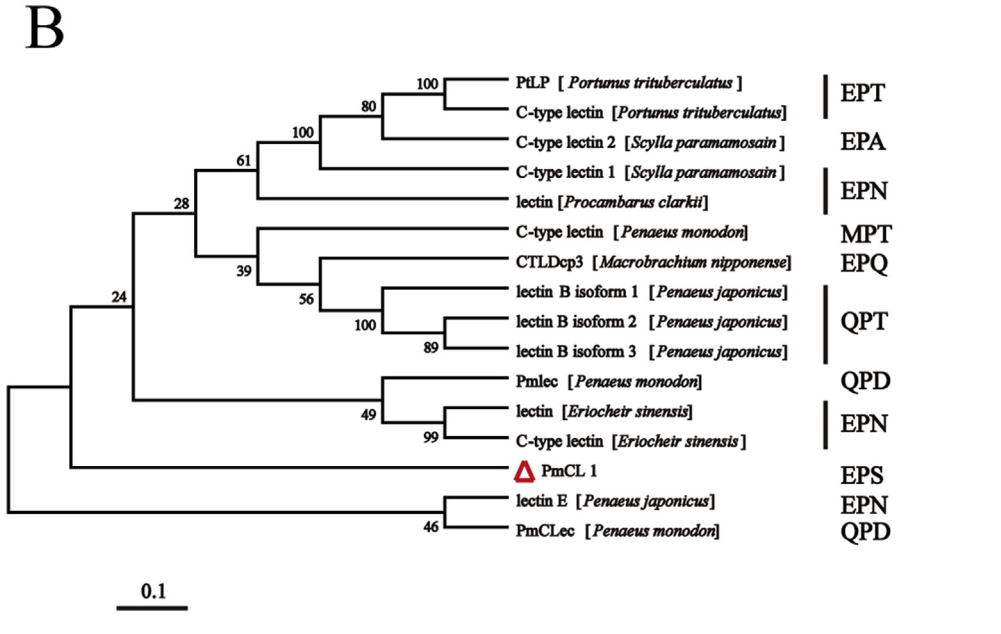

(caption on next page)

Fig. 2. Multiple alignment and phylogenetic analysis of *PmCL1*. (A) Multiple alignment of *PmCL1*. The sequence of *PmCL1* was aligned with similar genes from other species: *PtLP* (ACC86854.1), C-type lectin (AGH68927.1), C-type lectin 2 (AEO92002.1), C-type lectin 1 (AEO92001.1), lectin (ADB10837.1), C-type lectin (ADK66338.1), lectin E (ADG85658.1), lectin (AFJ11528.1), C-type lectin (DQ871244.1), Pmlec (DQ078266.1), *CTLDcp3* (ALF45199.1), lectin B isoform 1 (ADG85668.1), lectin B isoform 2 (ADG85661.1), and lectin B isoform 3 (ADG85660.1). Amino acid residues conserved in at least 85% of sequence are shaded in purple, and similarity at least 60% amino acids are shaded in blue. Conserved cysteine residues are marked with arrows. The CRD domain and the sugar-binding motif (EPS) are boxed. (B) Phylogenetic analysis of *PmCL1*. Two thousand bootstraps were performed on the neighbour-joining trees to check the repeatability of the results. *PmCL1* is marked by the red trilateral. (For interpretation of the references to colour in this figure legend, the reader is referred to the Web version of this article.)

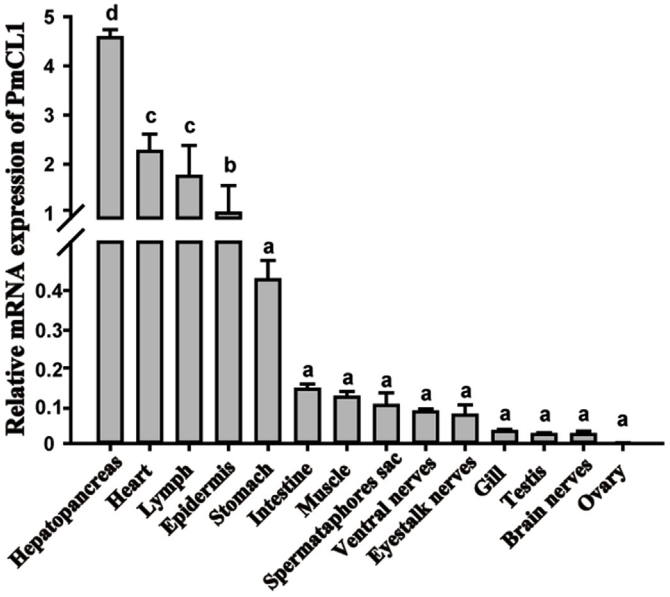

Fig. 3. *PmCL1* mRNA expression levels in different tissues. PmCL1 transcript levels in hepatopancreas, heart, lymph, gill, stomach, ventral nerves, muscle, spermataphore sac, intestine, eyestalk nerves, testis, brain nerves, and ovary, normalized to the epidermis. Vertical bars represent the mean ± S.E. (n = 3). The different letters denote significantly different expression ($P < 0.05$).

Almost all the bacteria in the field of vision were agglutinated after incubation with rPmCL1 and Ca^{2+}. Agglutination was markedly inhibited after the incubation of rPmCL1 in the PBS-Ca^{2+} buffer plus EDTA. A similar inhibitory effect was also observed in the presence of PGN (Fig. 8). The results confirmed that rPmCL1 could induce bacterial agglutination *in vitro*.

3.8. Bacterial clearance in vivo

To assess whether rPmCL1 could also agglutinate and clear invading bacteria *in vivo*, PBS, BSA, and rPmCL1 were incubated with *V. harveyi* before injection. The bacterial count in the haemolymph for the three experimental groups showed a downward trend. The bacterial numbers in the *V. harveyi* + rPmCL1 group were slightly lower than in the other groups, and no significant difference was observed at 5 min post-injection. The numbers of *V. harveyi* in the presence of rPmCL1 were reduced significantly at 15 min, and reached the lowest level at 30 min post-injection. Approximately 8.19×10^6 cfu/mL haemolymph remained in the rPmCL1 group, which was nearly half the bacterial density in the BSA group (1.64×107 cfu/mL) and the PBS group (1.50×10^7 cfu/mL) (Fig. 9). Thus, rPmCL1 could enhance the elimination of *V. harveyi* in tiger shrimp.

4. Discussion

The natural water environment represents a complex and ever-changing system. There is no clear consensus on the fact that environmental changes affect the immune system of crustacea [37]. As PRRs, lectins are important for the innate immunity against adverse environments in aquatic animals, including both fish [38,39] and crustaceans [16,22,25,40]. In the present study, a new CTL was identified from *P. monodon*. Tissue distribution analysis revealed the highest level of PmCL1 mRNA transcript in the hepatopancreas, whereas no transcripts were detected in the ovary. The expression levels of PmCL1 in the hepatopancreas and gill tissues were all significantly upregulated after stimulation by *V. harveyi* and *V. anguillarum*. Recombinant PmCL1 could induce the agglutination of bacteria *in vitro* and assist in the elimination of *V. harveyi in vivo*. In addition, the tolerance test results suggested that PmCL1 also responds to ammonia nitrogen.

Based on the results of sequence alignment and phylogenetic tree analysis, we designated the genes as PmCL1. A putative signal peptide was found in most CTLs, including PmCL1, suggesting that they were secreted out of the cells [41]. PmCL1 contains a single CRD domain, but with an EPS sugar-binding motif that was different from the known

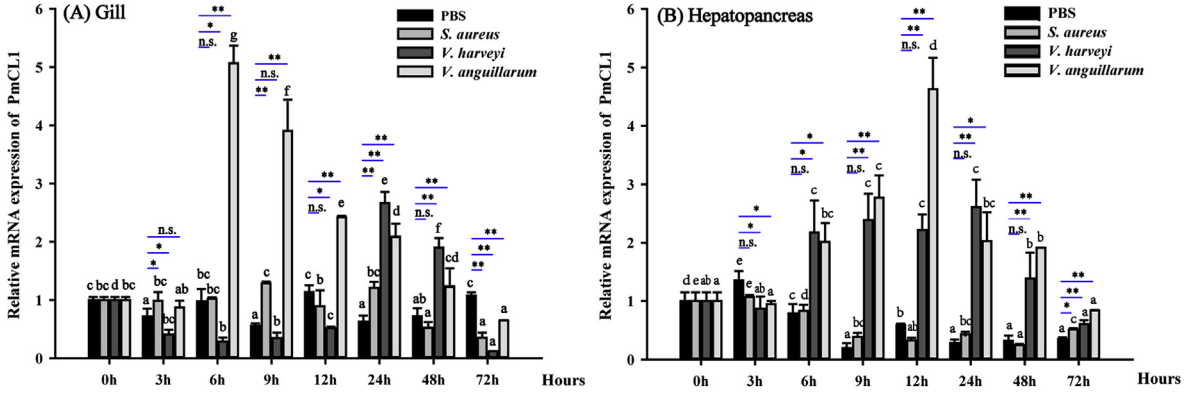

Fig. 4. Expression profiles of *PmCL1* after challenge with PBS, *V. harveyi*, *V. anguillarum*, and *S. aureus*. Samples challenged with PBS were the control and EF1α was the internal control. Total RNA extracted from gill (A) and hepatopancreas (B) of black tiger shrimp at different times after immune challenge. Significance was compared between the experimental groups and the control groups at the same time points. Significant differences are indicated by *($P < 0.05$) and **($P < 0.01$).

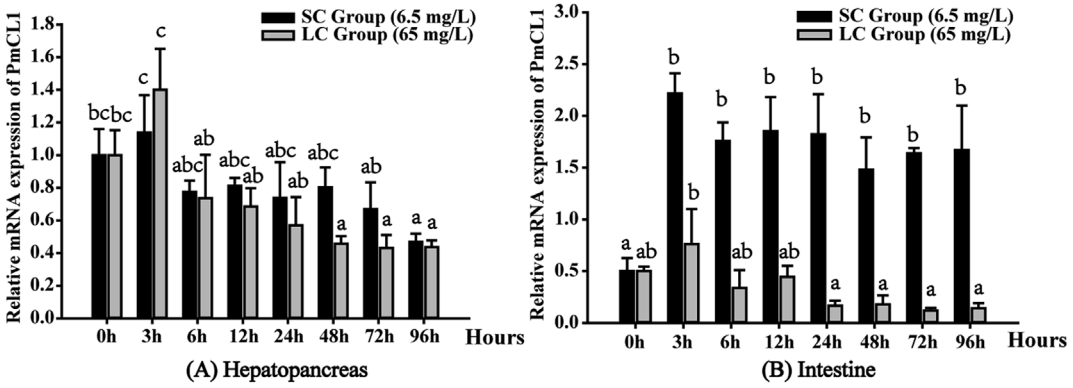

Fig. 5. mRNA expression levels of *PmCL1* in hepatopancreas (A) and intestines (B) at different times after SC50 and LC50 ammonia nitrogen treatment. EF1α was utilized as the internal reference gene. Vertical bars represent the mean ± SE (n = 3). The expression levels with different letters are significantly different ($P < 0.05$).

lectin from *P. monodon*, revealing a potentially different function of PmCL1. These calcium-binding sites coordinating calcium have different effects on the structure and function. Calcium-binding site 2 was involved in carbohydrate binding, which has been reported in some lectins [42–44]. Meanwhile, an abundant expression of PmCL1 was observed in hepatopancreas and lymph tissue, indicating its potential immune-related function like other lectins.

To test whether C-lectin participated in the host immune response against bacterial infection, shrimp were challenged with a gram-positive and 2 g-negative bacteria (*V. harveyi* and *V. anguillarum*). *V. harveyi* and *V. anguillarum* cause infections in cultivated shrimp that result in economic losses. Both gram-negative bacteria induced PmCL1 expression at 6 h in the hepatopancreas and gill samples. A previous study reported that *SpCTL-B* transcripts were increased significantly at 6 h in the hepatopancreas of *S. paramamosain*, when challenged by *V. parahemolyticus* [19]. This pattern revealed an acute response during the first few hours of the infection. Clearance occurred at 2–3 days post-infection, and was mediated by lectin and other immune molecules against the gram-negative bacteria. However, in the present study, the expression of PmCL1 after *S. aureus* challenge showed an increase only at 9 h post-infection in the gill tissue, and progressively decreased in the hepatopancreas tissue. The mRNA level of *MnCTL* was increased at 2, 6, and 12 h after *S. aureus* challenge [45]. These results suggest that PmCL1 could be stimulated by some bacteria and protect shrimp from further damage.

ELISA test was performed to analyse the rPmCL1 binding activity to PAMP and carbohydrates, in order to verify the role of PRR. The results clearly showed that rPmCL1 is an atypical PRR, with the highest sensitivity to PGN, followed by LPS, but no binding activity to LTA, which had some differences with other lectins. *MjLTL1* from *M. japonicus* had nearly the same binding specificity towards LPS, LTA, and PGN, except mannose [46]. *PcLec3* from *Procambarus clarkii* has an immunoglobulin-like domain, and it has been reported that rPcLec3 and rCTLD are both specific to three kinds of polysaccharides (PGN, LPS, and LTA) with different binding affinities [18]. Both PGN and LPS were effective PAMP that induce number of lectin expression on transcriptome level in Oyster *Crassostrea gigas* [47]. PGN is a polymer consisting of alternating residues of β-(1,4) linked N-acetylglucosamine (NAG)/N-acetylmuramic acid (NAM) and amino acids that form a mesh-like layer outside the plasma membrane of most bacteria. LPS consists of a lipid and a polysaccharide connected by a covalent bond, and is found only in the outer membrane of gram-negative bacteria, whereas LTA, containing ribitol or glycerol residues linked by phosphodiester bond, is found within the cell wall of most gram-positive bacteria. It appears that PmCL1 has a higher affinity to the polysaccharide residues of PGN and LPS compared with LTA, which was futher established with the qPCR result that PmCL1 was more sensitive to gram-negative bacteria than gram-positive bacteria.

Five types of saccharides were analysed by ELISA to test the binding activity to saccharide residues and all of them showed a high affinity to PmCL1. Three monosaccharides (α-lactose, D-glucose, and D-mannose) showed a higher affinity than glucose, treholose, and galactosamine. The differences in specificity to various carbohydrates were more dependent on the divergent sugar-binding motif. Some authors have reported that the binding specificity of the QAP motif was more similar to that of EPN than that of QPD. CTLDs with a QPD motif have an affinity for an equatorial/axial 3-OH/4-OH configuration of carbohydrate residues [48]. *Pmlec* from *P. monodon*, which contains the QPD motif, shows high affinity towards NeuAC, xylose, galatose, glucose, and maltose but a low affinity towards mannose and sucrose [23]. rMjGCTL

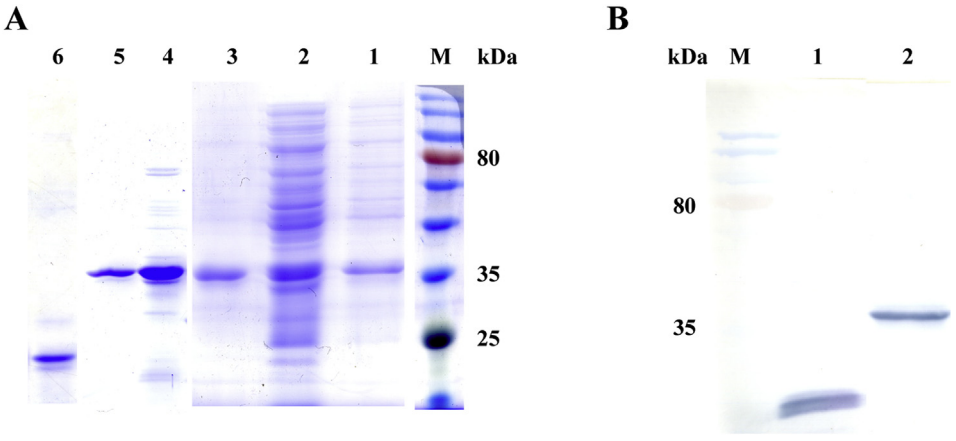

Fig. 6. SDS-PAGE and Western blot analysis of rPmCL1. (A) Lane M: standard protein marker; lane A1: total protein obtained from *E. coli* expressing pET32a-ORF after induction; lane A2: proteins in the supernatant after induction; lane A3: proteins in the sediment after induction; lane A4 and A5: purified recombinant PmCL1; and lane A6: purified pET32a empty plasmid; (B) Lane M: standard protein marker; lane B1: empty plasmid pET32a; and lane B2: rPmCL1.

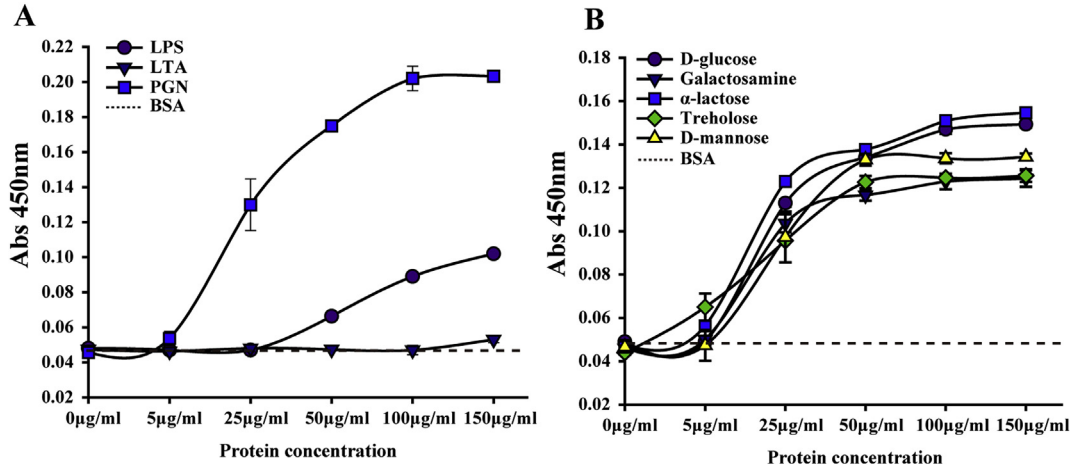

Fig. 7. ELISA analysis of the interaction between rPmCL1 to PAMPs (A) and saccharides (B). The microtiter plates were coated with 10 μg of PAMPs and saccharides, and then incubated with different concentrations of recombinant protein. The interaction between protein and PAMP/saccharides was detected by composite anti-His polyclonal antiserum at 450 nm. Results are representative of an average of three experiments.

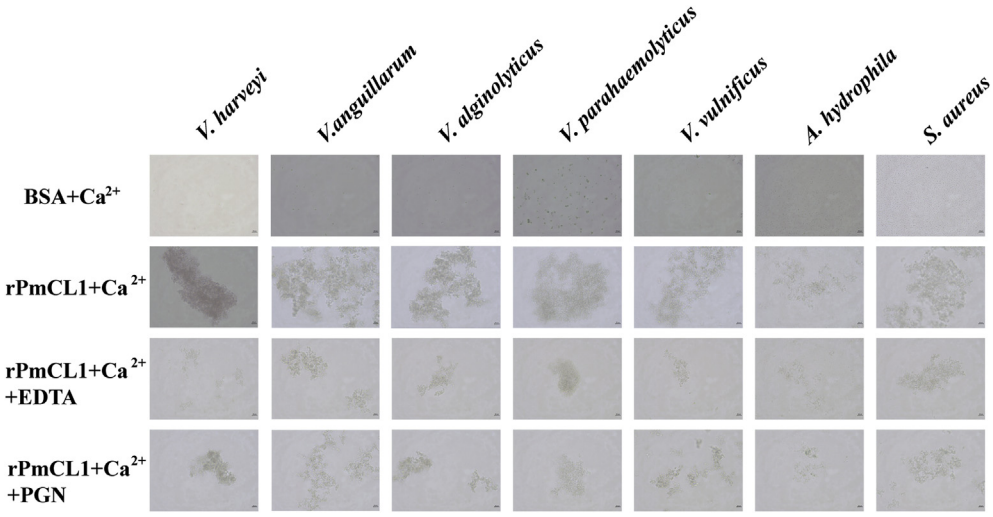

Fig. 8. Agglutination of bacteria by recombinant PmCL1 in a competitive agglutinating assay with Ca^{2+}. Gram-positive (*S. aureus*, 1×10^8 cfu/mL) and gram-negative bacteria (*V. harveyi*, *V. anguillarum*, *V. alginolyticus*, *V. parahemolyticus*, *V. vulnificus*, and *A. hydrophila*, 1×10^8 cfu/mL respectively) werewere treated with purified recombinant PmCL1 protein (2.5 μg) for 1 h in the presence of 10 mM $CaCl_2$ with or without EDTA at room temperature and examined under microscopy. PGN was resplace to EDTA as a competitive inhibitor to PmCL1. Negative control was added with BSA and $CaCl_2$.

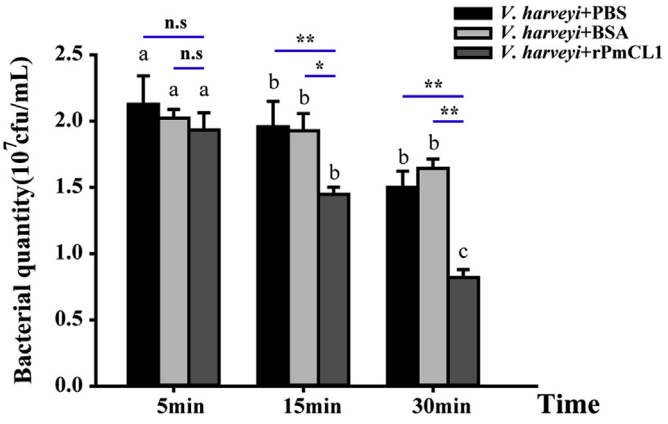

Fig. 9. *In vivo* bacterial clearance activities of PmCL1. Shrimp were injected with 1×10^7 cfu/mL *V. harveyi* pre-incubated with 500 μg/mL rPmCL1. Haemolymph was collected diluted, and plated on LB agar at different times after 5, 15 min or 30min post-injection. Plates were incubated at 28 °C for 12 h and bacteria were counted. Error barsrepresent ± SD of three replicates.

from *M. japonicus*, which has a QAP motif, does not bind to either D-mannose or D-galactose [49], thus, showing differences from rPmCL1, which has an EPS motif. PmCL1 seemed similar to the mannose binding lectin (MBL). MBL binds carbohydrates on the surface of microbial cells in a calcium-dependent manner, and opsonizes the pathogens for phagocytosis [42]. It indicated that PmCL1 may interact with the bacteria directly or indirectly.

Bacterial agglutination assay revealed that rPmCL1 could result in the agglutination of various bacteria in the presence of Ca^{2+}, which was likely determined by its structure. In silico analysis showed that PmCL1 contains a single CRD domain with six conserved cysteine residues. Structural analysis of the prototype CRD from serum mannose-binding protein showed that conserved residues ligate a Ca^{2+}, which forms the basis of a primary sugar-binding site [43]. The six conserved sites in PmCL1 might form the disulphide bond that exposes the binding side to Ca^{2+}, enabling the binding of sugars. PmCL1 showed a broad-spectrum bacterial aggregation activity, and strongly agglutinated most of the detected gram-negative bacterial pathogens of shrimp and a gram-positive bacteria. However, *PmCLec* [25], which contains a single CRD domain with four conserved cysteine residues, could bind gram-positive bacteria (*S. aureus*, *Streptococcus hemolyticus*) but not gram-negative bacteria (*Bacillus megaterium*, *V. harveyi*). Meanwhile, *PmLT* [24], which has two CRDs, could recognize viral pathogens and activate the immune response of the black tiger shrimp against bacteria. These results suggest that the number of CRD and location of cysteine residues might be associated with the binding ability towards bacteria.

Based on the bacterial agglutination results, *V. harveyi* was chosen

to analyse the bacterial clearance effect of PmCL1 *in vivo*. The results revealed that rPmCL1 could enhance the efficiency of clearing the invading bacteria. The bacterial counts in the test group, which was pre-incubated with rPmCL1, were significantly lower than those in the two control groups at 15 min after injection, suggesting an effective clearance in the test group. This suggested that PmCL1 plays a key role in first-line host defence, and that the autoimmune system was triggered in response to bacterial invasion. Lectins have been shown to act as PRRs for pathogen recognition, as well as opsonins, which promote the phagocytosis against invaders. MBL null mice were highly susceptible to *S. aureus* infection, and MBL-initiated opsonophagocytosis was effective in killing *S. aureus* [50]. A recent report confirmed that CTL1 from the amphioxus *B. belcheri* has the ability to recognize a wide range of microorganisms and directly kill microbes via interaction with peptidoglycan and glucan [51]. *SpCTL-B* can upregulate antimicrobial peptides and significantly enhance the phagocytosis ability of haemocytes in *S. paramamosain* [19]. PmCL1 is believed to cause microbial agglutination via interaction with PGN or LPS, while regulating the expression of antimicrobial peptides to enhance phagocytosis, thus, killing the invasive microbes.

On the other hand, ammonia nitrogen stress can also regulate the expression of PmCL1. We hypothesized that low concentration of ammonia can upregulate PmCL1 in the intestine, but the expression was finally reduced, not only in the hepatopancreas of the low ammonia group, but also in both tissues of the high ammonia group. These results were in accordance with our transcriptome results that indicated a downregulation of C-type lectin after ammonia exposure by Li [26]. Considering our previous results that ammonia may induce body immunity in the initial period, and then weaken it over prolonged stress duration, which not only inhibits the activity of immune enzymes, but also causes the downregulation of immune-related genes such as lysosome and crustin during the later stage [31], and our recent RNA-seq results that apoptosis pathway is activated with a concurrent downregulation of many immune-related genes, we predicted that high ammonia stress might destroy the innate immunity and induce apoptosis in shrimp. Furthermore, ammonia can have a profound effect on the display of cell-surface carbohydrate epitopes, thus, preventing the translocation of secretory proteins such as CTLs and lysozyme to the cell periphery [52,53], which may ultimately cause a decrease in haemocyte numbers [54] and morphological changes in hepatopancreas (data not shown), with the detailed underlying mechanisms requiring further research.

In conclusion, PmCL1, a member of CTL superfamily, was upregulated by bacterial infection, and displayed as a PRR that ensured specific binding to various PAMPs and carbohydrates, except LTA. At the same time, rPmCL1 induced bacterial agglutination and enhanced the efficiency of bacterial clearance. In addition, PmCL1 was inhibited when shrimp experienced high concentrations of ammonia nitrogen. Future studies are needed to clarify the underlying immunological mode-of-action of PmCL1.

Acknowledgements

This study was funded by Special Support for young talent with scientific and technological innovation of Guangdong Province (2015TQ01N583), China agriculture research system (CARS-48), Special fund for the Development of marine fishery scientific technology and industry of Guangdong Province (A201701A01), Special fund for economic development of Guangdong Province in 2018 (Guangdong Fishery 2018-02), Development of Biology industry in Shenzhen (JCYJ20170412110605075).

Appendix A. Supplementary data

Supplementary data to this article can be found online at https://doi.org/10.1016/j.fsi.2019.04.034.

References

[1] A.F. Rowley, A. Powell, Invertebrate immune systems-specific, quasi-specific, or nonspecific? J. Immunol. 179 (11) (2007) 7209–7214.
[2] L.E. S, A.C. M, Z. Si-Ming, K.T. B, Invertebrate immune systems – not homogeneous, not simple, not well understood, Immunol. Rev. 198 (1) (2004) 10–24.
[3] R. Medzhitov, Decoding the patterns of self and nonself by the innate immune system, Science 296 (5566) (2002) 298–300.
[4] L.-S. Yang, Z.-X. Yin, J.-X. Liao, X.-D. Huang, C.-J. Guo, S.-P. Weng, S.-M. Chan, X.-Q. Yu, J.-G. He, A Toll receptor in shrimp, Mol. Immunol. 44 (8) (2007) 1999–2008.
[5] Q. Liu, D. Xu, S. Jiang, J. Huang, F. Zhou, Q. Yang, S. Jiang, L. Yang, Toll-receptor 9 gene in the black tiger shrimp (*Penaeus monodon*) induced the activation of the TLR–NF-κB signaling pathway, Gene 639 (2018) 27–33.
[6] L. Peiser, S. Mukhopadhyay, S. Gordon, Scavenger receptors in innate immunity, Curr. Opin. Immunol. 14 (1) (2002) 123–128.
[7] M. Li, C. Li, C. Ma, H. Li, H. Zuo, S. Weng, X. Chen, D. Zeng, J. He, X. Xu, Identification of a C-type lectin with antiviral and antibacterial activity from pacific white shrimp *Litopenaeus vannamei*, Dev. Comp. Immunol. 46 (2) (2014) 231–240.
[8] G.R. Vasta, C. Feng, N. González-Montalbán, J. Mancini, L. Yang, K. Abernathy, G. Frost, C. Palm, Functions of galectins as 'self/non-self'-recognition and effector factors, Pathogens and Disease 75 (5) (2017).
[9] X.W. Wang, X.F. Zhao, J.X. Wang, C-type lectin binds to beta-integrin to promote hemocytic phagocytosis in an invertebrate, J. Biol. Chem. 289 (4) (2014) 2405–2414.
[10] B. Beutler, Innate immunity: an overview, Mol. Immunol. 40 (12) (2004) 845–859.
[11] X.-W. Wang, J.-X. Wang, Diversity and multiple functions of lectins in shrimp immunity, Dev. Comp. Immunol. 39 (1) (2013) 27–38.
[12] A.N. Zelensky, J.E. Gready, The C-type lectin-like domain superfamily, FEBS J. 272 (24) (2005) 6179–6217.
[13] W.W. I, T.M. E, D. Kurt, The C-type lectin superfamily in the immune system, Immunol. Rev. 163 (1) (1998) 19–34.
[14] K. Nobuo, I. Morikazu, K. Tomoyuki, Y. Katsuro, I. Hidenori, S. Ryoichi, The lipopolysaccharide-binding protein participating in hemocyte nodule formation in the silkworm *Bombyx mori* is a novel member of the C-type lectin superfamily with two different tandem carbohydrate-recognition domains 1, FEBS (Fed. Eur. Biochem. Soc.) Lett. 443 (2) (1999) 139–143.
[15] G.K. Christophides, E. Zdobnov, C. Barillas-Mury, E. Birney, S. Blandin, C. Blass, P.T. Brey, F.H. Collins, A. Danielli, G. Dimopoulos, C. Hetru, N.T. Hoa, J.A. Hoffmann, S.M. Kanzok, I. Letunic, E.A. Levashina, T.G. Loukeris, G. Lycett, S. Meister, K. Michel, L.F. Moita, H.M. Muller, M.A. Osta, S.M. Paskewitz, J.M. Reichhart, A. Rzhetsky, L. Troxler, K.D. Vernick, D. Vlachou, J. Volz, C. von Mering, J. Xu, L. Zheng, P. Bork, F.C. Kafatos, Immunity-related genes and gene families in *Anopheles gambiae*, Science 298 (5591) (2002) 159–165.
[16] X.W. Wang, X.W. Zhang, W.T. Xu, X.F. Zhao, J.X. Wang, A novel C-type lectin (FcLec4) facilitates the clearance of *Vibrio anguillarum in vivo* in Chinese white shrimp, Dev. Comp. Immunol. 33 (9) (2009) 1039–1047.
[17] M.J. Robinson, D. Sancho, E.C. Slack, S. LeibundGut-Landmann, C. Reis e Sousa, Myeloid C-type lectins in innate immunity, Nat. Immunol. 7 (12) (2006) 1258–1265.
[18] X.W. Zhang, Y. Wang, X.W. Wang, L. Wang, Y. Mu, J.X. Wang, A C-type lectin with an immunoglobulin-like domain promotes phagocytosis of hemocytes in crayfish *Procambarus clarkii*, Sci. Rep. 6 (2016) 29924.
[19] X. Wei, L. Wang, W. Sun, M. Zhang, H. Ma, Y. Zhang, X. Zhang, S. Li, C-type lectin B (SpCTL-B) regulates the expression of antimicrobial peptides and promotes phagocytosis in mud crab *Scylla paramamosain*, Dev. Comp. Immunol. 84 (2018) 213–229.
[20] X. Zhang, J. Lu, C. Mu, R. Li, W. Song, Y. Ye, C. Shi, L. Liu, C. Wang, Molecular cloning of a C-type lectin from *Portunus trituberculatus*, which might be involved in the innate immune response, Fish Shellfish Immunol. 76 (2018) 216–223.
[21] Y. Huang, L. An, K.M. Hui, Q. Ren, W. Wang, An LDLa domain-containing C-type lectin is involved in the innate immunity of *Eriocheir sinensis*, Dev. Comp. Immunol. 42 (2) (2014) 333–344.
[22] Y. Xiu, Y. Wang, J. Bi, Y. Liu, M. Ning, H. Liu, S. Li, W. Gu, W. Wang, Q. Meng, A novel C-type lectin is involved in the innate immunity of *Macrobrachium nipponense*, Fish Shellfish Immunol. 50 (2016) 117–126.
[23] T. Luo, H. Yang, F. Li, X. Zhang, X. Xu, Purification, characterization and cDNA cloning of a novel lipopolysaccharide-binding lectin from the shrimp *Penaeus monodon*, Dev. Comp. Immunol. 30 (7) (2006) 607–617.
[24] T.H. Ma, J.A. Benzie, J.G. He, S.M. Chan, PmLT, a C-type lectin specific to hepatopancreas is involved in the innate defense of the shrimp *Penaeus monodon*, J. Invertebr. Pathol. 99 (3) (2008) 332–341.
[25] R. Wongpanya, P. Sengprasert, P. Amparyup, A. Tassanakajon, A novel C-type lectin in the black tiger shrimp *Penaeus monodon* functions as a pattern recognition receptor by binding and causing bacterial agglutination, Fish Shellfish Immunol. 60 (2017) 103–113.
[26] Y. Li, F. Zhou, J. Huang, L. Yang, S. Jiang, Q. Yang, J. He, S. Jiang, Transcriptome reveals involvement of immune defense, oxidative imbalance, and apoptosis in ammonia-stress response of the black tiger shrimp (*Penaeus monodon*), Fish Shellfish Immunol. 83 (2018) 162–170.
[27] M. de Lourdes Cobo, S. Sonnenholzner, M. Wille, P. Sorgeloos, Ammonia tolerance of *Litopenaeus vannamei* (Boone) larvae, Aquacult. Res. 45 (3) (2014) 470–475.
[28] J.-C. Chen, C.-Y. Lin, Lethal effects of ammonia on *Penaeus chinensis* Osbeck juveniles at different salinity levels, J. Exp. Mar. Biol. Ecol. 156 (1) (1992) 139–148.
[29] J.-C. Chen, P.-C. Liu, S.-C. Lei, Toxicities of ammonia and nitrite to *Penaeus monodon* adolescents, Aquaculture 89 (2) (1990) 127–137.

[30] A. Ostrensky, W. Wasielesky, Acute toxicity of ammonia to various life stages of the São Paulo shrimp, Penaeus paulensis Pérez-Farfante, 1967, Aquaculture 132 (3) (1995) 339–347.
[31] L. Yang, Q. Yang, S. Jiang, Y. Li, F. Zhou, T. Li, J. Huang, Metabolic, immune responses in prawn (*Penaeus monodon*) exposed to ambient ammonia, Aquacult. Int. 23 (4) (2014) 1049–1062.
[32] X. Wang, L. Wang, C. Yao, L. Qiu, H. Zhang, Z. Zhi, L. Song, Alternation of immune parameters and cellular energy allocation of *Chlamys farreri* under ammonia-N exposure and *Vibrio anguillarum* challenge, Fish Shellfish Immunol. 32 (5) (2012) 741–749.
[33] M. Hong, L. Chen, X. Sun, S. Gu, L. Zhang, Y. Chen, Metabolic and immune responses in Chinese mitten-handed crab (*Eriocheir sinensis*) juveniles exposed to elevated ambient ammonia, Comp. Biochem. Physiol. C Toxicol. Pharmacol. 145 (3) (2007) 363–369.
[34] X. Lu, J. Kong, S. Luan, P. Dai, X. Meng, B. Cao, K. Luo, Transcriptome analysis of the hepatopancreas in the pacific white shrimp (*Litopenaeus vannamei*) under acute ammonia stress, PLoS One 11 (10) (2016) e0164396.
[35] D. Zhu, L. Yang, H. Jianhua, Z. Falin, Y. Qibin, J. Song, S. Jiang, The Comprehensive Expression Analysis of the G Protein-Coupled Receptor from Penaeus monodon Indicating it Participates in Innate Immunity and Anti-ammonia Nitrogen Stress, Fish Shellfish Immunol, 2018.
[36] L. Yang, X. Liu, W. Liu, X. Li, L. Qiu, J. Huang, S. Jiang, Characterization of complement 1q binding protein of tiger shrimp, *Penaeus monodon*, and its C1q binding activity, Fish Shellfish Immunol. 34 (1) (2013) 82–90.
[37] G. Le Moullac, P. Haffner, Environmental factors affecting immune responses in Crustacea, Aquaculture 191 (1) (2000) 121–131.
[38] M. Zhang, Y.H. Hu, L. Sun, Identification and molecular analysis of a novel C-type lectin from *Scophthalmus maximus*, Fish Shellfish Immunol. 29 (1) (2010) 82–88.
[39] S. Russell, J.S. Lumsden, Function and heterogeneity of fish lectins, Vet. Immunol. Immunopathol. 108 (1–2) (2005) 111–120.
[40] L. Wang, L. Wang, D. Zhang, F. Li, M. Wang, M. Huang, H. Zhang, L. Song, A novel C-type lectin from crab *Eriocheir sinensis* functions as pattern recognition receptor enhancing cellular encapsulation, Fish Shellfish Immunol. 34 (3) (2013) 832–842.
[41] Y.-H. Xu, W.-J. Bi, X.-W. Wang, Y.-R. Zhao, X.-F. Zhao, J.-X. Wang, Two novel C-type lectins with a low-density lipoprotein receptor class A domain have antiviral function in the shrimp *Marsupenaeus japonicus*, Dev. Comp. Immunol. 42 (2) (2014) 323–332.
[42] D.L. Jack, N.J. Klein, M.W. Turner, Mannose-binding lectin: targeting the microbial world for complement attack and opsonophagocytosis, Immunol. Rev. 180 (1) (2001) 86–99.
[43] W.I. Weis, K. Drickamer, W.A. Hendrickson, Structure of a C-type mannose-binding protein complexed with an oligosaccharide, Nature 360 (1992) 127.
[44] J. Yang, L. Wang, H. Zhang, L. Qiu, H. Wang, L. Song, C-type lectin in *Chlamys farreri* (CfLec-1) mediating immune recognition and opsonization, PLoS One 6 (2) (2011) e17089.
[45] X. Huang, T. Li, M. Jin, S. Yin, W. Wang, Q. Ren, Identification of a *Macrobrachium nipponense* C-type lectin with a close evolutionary relationship to vertebrate lectins, Mol. Immunol. 87 (2017) 141–151.
[46] S. Xu, L. Wang, X.W. Wang, Y.R. Zhao, W.J. Bi, X.F. Zhao, J.X. Wang, L-Type lectin from the kuruma shrimp *Marsupenaeus japonicus* promotes hemocyte phagocytosis, Dev. Comp. Immunol. 44 (2) (2014) 397–405.
[47] L. Wang, H. Zhang, M. Wang, Z. Zhou, W. Wang, R. Liu, M. Huang, C. Yang, L. Qiu, L. Song, The transcriptomic expression of pattern recognition receptors: insight into molecular recognition of various invading pathogens in Oyster *Crassostrea gigas*, Dev. Comp. Immunol. 91 (2018) 1–7.
[48] A.R. Kolatkar, W.I. Weis, Structural basis of galactose recognition by C-type animal lectins, J. Biol. Chem. 271 (12) (1996) 6679–6685.
[49] R.R.R. Alenton, K. Koiwai, K. Miyaguchi, H. Kondo, I. Hirono, Pathogen recognition of a novel C-type lectin from *Marsupenaeus japonicus* reveals the divergent sugar-binding specificity of QAP motif, Sci. Rep. 7 (2017) 45818.
[50] P.D. Stahl, R.A.B. Ezekowitz, The mannose receptor is a pattern recognition receptor involved in host defense, Curr. Opin. Immunol. 10 (1) (1998) 50–55.
[51] G. Huang, A. Xu, Chapter 9 - immune effectors in amphioxus, in: A. Xu (Ed.), Amphioxus Immunity, Academic Press 2016, pp. 167-188.
[52] P.O. Seglen, A. Reith, Ammonia inhibits protein secretion in isolated rat hepatocytes, Biochim. Biophys. Acta Gen. Subj. 496 (1) (1977) 29–35.
[53] J.A. Zanghi, T.P. Mendoza, R.H. Knop, W.M. Miller, Ammonia inhibits neural cell adhesion molecule polysialylation in Chinese hamster ovary and small cell lung cancer cells, J. Cell. Physiol. 177 (2) (1998) 248–263.
[54] T. Rodríguez-Ramos, G. Espinosa, J. Hernández-López, T. Gollas-Galván, J. Marrero, Y. Borrell, M.E. Alonso, U. Bécquer, M. Alonso, Effects of Echerichia coli lipopolysaccharides and dissolved ammonia on immune response in southern white shrimp *Litopenaeus schmitti*, Aquaculture 274 (1) (2008) 118–125.